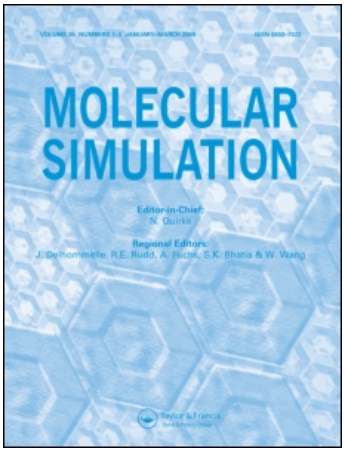

Molecular Simulation
Publication details, including instructions for authors and subscription information:
http://www.informaworld.com/smpp/title~content=t713644482

Analysis of dissociation process for gas hydrates by molecular dynamics simulation

Yoshio Iwai[a]; Hiroki Nakamura[a]; Yuki Arai[a]; Yusuke Shimoyama[a]
[a] Department of Chemical Engineering, Kyushu University, Fukuoka, Japan

First published on: 08 October 2009

To cite this Article Iwai, Yoshio , Nakamura, Hiroki , Arai, Yuki and Shimoyama, Yusuke(2010) 'Analysis of dissociation process for gas hydrates by molecular dynamics simulation', Molecular Simulation, 36: 3, 246 — 253, First published on: 08 October 2009 (iFirst)
To link to this Article: DOI: 10.1080/08927020903307529
URL: http://dx.doi.org/10.1080/08927020903307529

Molecular Simulation
Vol. 36, No. 3, March 2010, 246–253

Taylor & Francis
Taylor & Francis Group

Analysis of dissociation process for gas hydrates by molecular dynamics simulation

Yoshio Iwai*, Hiroki Nakamura, Yuki Arai and Yusuke Shimoyama

Department of Chemical Engineering, Kyushu University, 744 Motooka, Nishi-ku, Fukuoka 819-8581, Japan

(*Received 4 March 2009; final version received 3 September 2009*)

The dissociation processes of methane and carbon dioxide hydrates were investigated by molecular dynamics simulation. The simulations were performed with 368 water molecules and 64 gas molecules using *NPT* ensembles. The TraPPE (single-site) and 5-site models were adopted for methane molecules. The EPM2 (3-site) and SPC/E models were used for carbon dioxide and water molecules, respectively. The simulations were carried out at 270 K and 5.0 MPa for hydrate stabilisation. Then, temperature was increased up to 370 K. The temperature increasing rates were 0.1–20 TK/s. The gas hydrates dissociated during increasing temperature or at 370 K. The potential models of methane molecule did not much influence the dissociation process of methane hydrate. The mechanisms of dissociation process were analysed with the coordination numbers and mean square displacements. It was found that the water cages break down first, then the gas molecules escape from the water cages. The methane hydrate was more stable than the carbon dioxide hydrate at the calculated conditions.

Keywords: molecular dynamics simulation; methane hydrate; carbon dioxide hydrate; dissociation process

1. Introduction

Recently, gas hydrates have been receiving special attention in environmental and energy resource problems. When the guest molecules are methane (CH_4) and carbon dioxide (CO_2), they are called CH_4 and CO_2 hydrates, respectively. The gas hydrate is a solid-like crystalline and water molecules (host molecules) are linked through hydrogen bonding to form a lattice structure with cavities in which gas molecules (guest molecules) are included. The CH_4 and CO_2 hydrates belong to type I hydrate [1]. The crystal structure of type I in a unit cell consists of six middle cages (tetrakaidecahedra) and two small cages (pentagonal dodecahedra), where these eight cages consist of 46 H_2O molecules. The total amount of methane stored in CH_4 hydrate is estimated to be enormous. Methane hydrate is considered as a future energy resource. The storage and transportation of CH_4 gas can be changed from LNG to CH_4 hydrate because of economic advantages. The idea to store up CO_2 on the ocean floor in the form of CO_2 hydrate was proposed to keep the concentration of CO_2 in the air below a given level. However, the thermodynamic properties and the kinetics of the gas hydrates have not yet been well accumulated, because the experimental research to elucidate their molecular level structures is hard.

Hirai et al. [2] studied the stability of the CO_2 hydrate using molecular dynamics (MD) simulation. They reported that the CO_2 hydrate is unstable as compared with both empty and argon hydrates because the repulsive force acting between O atoms of CO_2 and O atoms in H_2O has a destabilising effect on the CO_2 hydrate lattice structure. Hirai et al. [3] performed CO_2 hydrate formation by MD simulation. Tse and Klug [4] investigated the formation and decomposition mechanisms for hydrates. They reported that the preservation effect may be explained with a phenomenological model assuming the formation of a thin ice crust layer. Chialvo et al. [5] studied the structures and thermophysical properties of CH_4 and CO_2 hydrates by MD simulation with several molecular models. English et al. [6] calculated the decomposition of CH_4 hydrate by MD simulation at 276.65 K and 68 bar. They indicated that the diffusion of methane molecules to the surrounding liquid layer from the crystal surface appears to be the rate-controlling step in hydrate breakup. Ding et al. [7] studied CH_4 hydrate dissociation process by MD simulation at constant temperatures. They found that the first stage is the process associated with diffusive behaviour of host molecules, and methane molecules escape from the broken cavities. Myshakin et al. [8] also investigated the decomposition of CH_4 hydrate by MD simulation at constant temperatures. It was found that reversible formation of partial water cages around methane molecules in liquid was observed at the interface at temperatures above the computed hydrate decomposition temperature. In the literature shown above, the dissociation processes for CH_4 hydrate were investigated by MD simulation at constant temperatures.

In this work, the dissociation processes for CH_4 and CO_2 hydrates were investigated by MD simulation with increasing temperature. The decomposition mechanism was analysed from the coordination numbers and mean square displacements for CH_4 and CO_2 hydrates.

*Corresponding author. Email: iwai@chem-eng.kyushu-u.ac.jp

ISSN 0892-7022 print/ISSN 1029-0435 online

DOI: 10.1080/08927020903307529
http://www.informaworld.com

Table 1. Potential parameters and charges.

Site (model)	ε/k (K)	σ (nm)		
Water			q_H (e)	q_O (e)
O (SPC/E)[a]	78.23	0.3166	+0.4238	−0.8476
Methane				
CH_4 (TraPPE)[b]	148.0	0.3730		
CC (5-site)[c]	48.72	0.3351		
CH (5-site)[c]	20.55	0.3024		
HH (5-site)[c]	6.79	0.2868		
Carbon dioxide			q_C (e)	q_O (e)
C (EPM2)[d]	28.13	0.2757	+0.6512	
O (EPM2)[d]	80.51	0.3033		−0.3256

[a] The SPC/E potential model [15] is used for water.
[b] The TraPPE model [13] is used for the single-site model of methane.
[c] The 5-site model [5] is used for methane.
[d] The EPM2 [14] model is used for carbon dioxide.

2. Simulation condition

The software used for the MD calculations was WinMASPHYCPro2.2 produced by Fujitsu. The general MD calculation conditions adopted in this work are as follows:

(1) Boundary condition: periodic boundary condition;
(2) Temperature control: Nose method [9];
(3) Pressure control: Parrinello–Rahman method [10];
(4) Time step: 1 fs and
(5) Potential cut: half of the initial cell length.

The densities of pure methane were calculated to compare the potential models of methane. The calculations were performed with 256 molecules of methane at 5.0 MPa and 370 K.

The calculation conditions for hydrates are as follows:

(1) Number of unit cells: 8 (unit cell consists of 46 water and 8 guest molecules);
(2) Initial coordinate: the initial coordinates of the molecules were determined from the crystal structure obtained by the neutron-ray diffraction experiments [11];
(3) Ensemble: *NPT* {*N*, number of particles (water molecules 368, gas molecules 64); *P*, pressure (5.0 MPa); *T*, temperature};
(4) Temperature profile: equilibrium calculation at 270 K for 100 ps, temperature increasing rates $\Delta T = 0.1$ to 20 TK/s up to 370 K and
(5) Long-range electrostatic interactions: Ewald method [12].

3. Potential

The TraPPE [13] and 5-site [5] models were adopted for methane to compare the effect of potential models. The TraPPE is a sphere model. The volume of hydrogen in the methane molecule is not so large that the approximation of the sphere model may be reasonable for methane to reduce the calculation times. The 5-sites model is a more realised model for methane. For carbon dioxide, the EPM2 [14] model was used for the calculations. The EPM2 is a 3-site model which gives reasonable saturated lines and heat of vaporisation of carbon dioxide. The SPC/E [15] model was adopted for water. The SPC/E model gives reasonable saturated lines and radial distribution function for water [16]. The calculated results of the Henry constants for methane in water agree well with the experimental data with the potential set of the SPC/E model for water and the TraPPE model for methane [17].

The intermolecular interaction ϕ_{ij} between molecules i and j was calculated by the Lennard-Jones potential coupled with the Coulomb interaction shown in Equation (1):

$$\phi_{ij} = \sum_s \sum_t 4\varepsilon_{st}\left[\left(\frac{\sigma_{st}}{r_{st}}\right)^{12} - \left(\frac{\sigma_{st}}{r_{st}}\right)^{6}\right] + \frac{e^2}{4\pi\varepsilon_0}\sum_s\sum_t \frac{q_s q_t}{r_{st}}, \tag{1}$$

where r is the distance of sites, ε_{st} and σ_{st} are the energy and size parameters, respectively, and subscripts s and t denote sites s and t, respectively, e is the elementary charge, ε_0 is the permittivity of free space and q is the charge. The values of the parameters are listed in Table 1. The Lorentz–Berthelot combining rule shown in Equation (2) was adopted between different sites

$$\varepsilon_{st} = \sqrt{\varepsilon_s \varepsilon_t}, \quad \sigma_{st} = \frac{\sigma_s + \sigma_t}{2}. \tag{2}$$

4. Analysis methods

The radial distribution function, coordination number and mean square displacement were adopted to analyse the dissociation process of hydrates. The definitions of the methods are shown by the following equations.

The radial distribution function $g_{st}(r)$ is defined by

$$g_{st}(r) = \frac{V}{N_s N_t}\sum_k^{N_s} \frac{n_{kt}}{4\pi r^2 \Delta r}, \tag{3}$$

where N is the number of sites in the system, V is the volume of the cell and n is the number of sites included in the spherical shell of Δr in thickness at r position.

The coordination number $Z_{sj}(r)$ is defined by the following equation:

$$Z_{st}(r) = \sum_n \frac{N_t}{V} g_{st}(n \cdot \Delta r). \tag{4}$$

The mean square displacement L_{MSD} is defined by

$$L_{MSD} = \frac{1}{N_i}\sum_{i}^{N_i} |r_i(t) - r_i(t_0)|^2, \quad (5)$$

where $r_i(t) - r_i(t_0)$ is the displacement of molecule i from time t_0 to t.

5. Results and discussion

5.1 Comparison of potential models of methane

The densities of methane were calculated with the TraPPE (single-site) and 5-site models at 5.0 MPa and 370 K. The simulations were carried out for 60 ps to reach the equilibrium conditions and the results from 60 to 100 ps were averaged to determine the densities of methane. The densities were 27.5 and 26.6 kg/m^3 with the TraPPE and 5-site models, respectively. The calculated value with a precise equation of state is 26.907 kg/m^3 at the same condition [18]. Both the potentials give reasonable values for the densities of methane. Figure 1 shows the calculated results of methane–methane and carbon atom–carbon atom radial distribution functions at 5.0 MPa and 370 K with the TraPPE and 5-site models, respectively. As shown in Figure 1, the positions of the first peaks with two potentials are almost the same. The initial rise of radial distribution function with the TraPPE model is slightly sharper than that with the 5-site model. The height of the radial distribution function with the TraPPE model is slightly higher than that with the 5-site model. The results mean that the molecules of the TraPPE model are slightly easier to be close to each other when compared with those of the 5-site model.

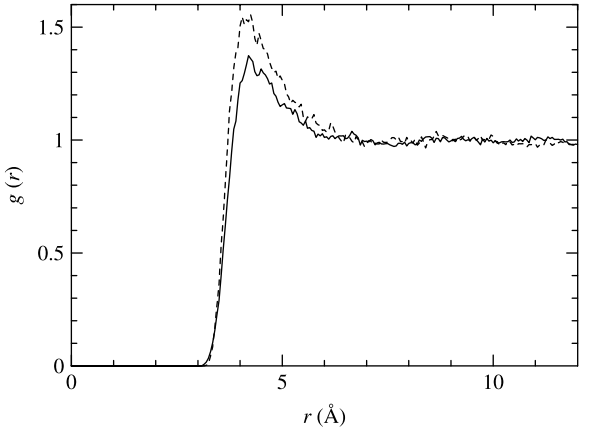

Figure 1. Radial distribution functions of methane at 5.0 MPa and 370 K; (—) carbon atom–carbon atom with the 5-site model; (- - -) methane–methane with the TraPPE model.

5.2 Temperature profiles and cell lengths

The temperature profiles and cell lengths are shown in Figure 2 for CH_4 and CO_2 hydrates. In this figure, the meaning of marks written in the left and upper sides is as follows: M and C mean CH_4 and CO_2 hydrates, respectively, the values after hyphen are the increasing rate of temperature in the unit of TK/s and the potential models of guest molecules are shown in parentheses. The marks are used for all of the following figures in this work. In the case of low increasing rate of temperature such as 0.1 TK/s, the cell lengths slowly increased with increasing temperature, and rapidly increased during increasing temperature. In the case of high increasing rate of temperature such as 20 TK/s, the cell length increased as the temperature increased, and the cell lengths rapidly increased at 370 K. When the cell length increased rapidly, the hydrate dissociated. The dissociate temperatures and cell lengths of methane are shown in Figure 2(b) and (c) with two potential models. The dissociate time of methane with the TraPPE model was slightly slower than that with the 5-site model. The cell lengths at 270 K were very similar to the two potential models. The cell length and structure of the hydrate are dependent on the potential model of host water molecules, and are almost independent of the potentials of guest molecules. After dissociation, the cell length with the TraPPE model was 26.5 Å and that with the 5-site model was 28.5 Å. The cell lengths after dissociation were influenced by the potential models between water and methane molecules. The dissociate temperature depends on the increasing rate of temperature. For example, the dissociate temperatures for CO_2 hydrate were about 320 and 350 K for $\Delta T = 0.1$ and 0.5 TK/s, respectively. The dissociation time and temperature of CO_2 hydrate were faster and lower than those for CH_4 hydrate with the two potential models for each increasing rate of temperature, respectively. This means that CH_4 hydrate was more stable than CO_2 hydrate at the calculated conditions with the potentials adopted in this work.

5.3 Snapshots of methane hydrate

Figure 3 shows three snapshots of CH_4 hydrate. Figure 3(a) shows the equilibrium state at 270 K. It can be confirmed that the molecules constitute the hydrate structure. During increasing temperature, the hydrate maintained the structure for a while, and then it began to decompose. Figure 3(b) shows the configuration in the middle of decomposition. Figure 3(c) shows the configuration at 370 K. The hydrate structure cannot be observed and the system was separated into CH_4- and H_2O-rich phases.

5.4 Radial distribution function

Figure 4 shows the radial distribution functions for M-0.5. As shown in Figure 4(a) at 270 K, the first peaks of the

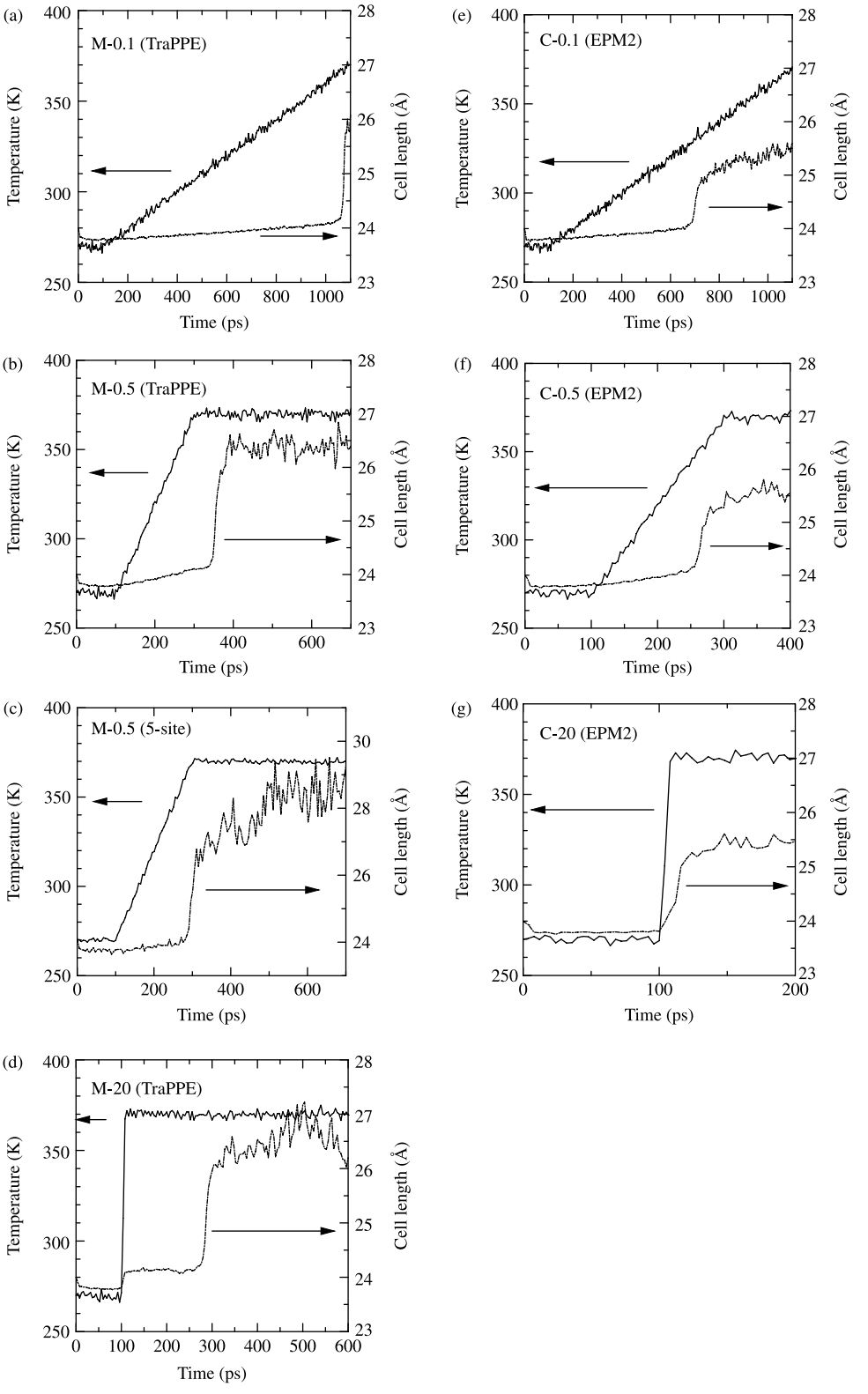

Figure 2. Temperature profiles and cell lengths for CH_4 and CO_2 hydrates. (a) CH_4 hydrate with the TraPPE model, $\Delta T = 0.1$ TK/s; (b) CH_4 hydrate with the TraPPE model, $\Delta T = 0.5$ TK/s; (c) CH_4 hydrate with the 5-site model, $\Delta T = 0.5$ TK/s; (d) CH_4 hydrate with the TraPPE model, $\Delta T = 20$ TK/s; (e) CO_2 hydrate with the EPM2 model, $\Delta T = 0.1$ TK/s; (f) CO_2 hydrate with the EPM2 model, $\Delta T = 0.5$ TK/s and (g) CO_2 hydrate with the EPM2 model, $\Delta T = 20$ TK/s; (—) temperature profile; (- - -) cell length.

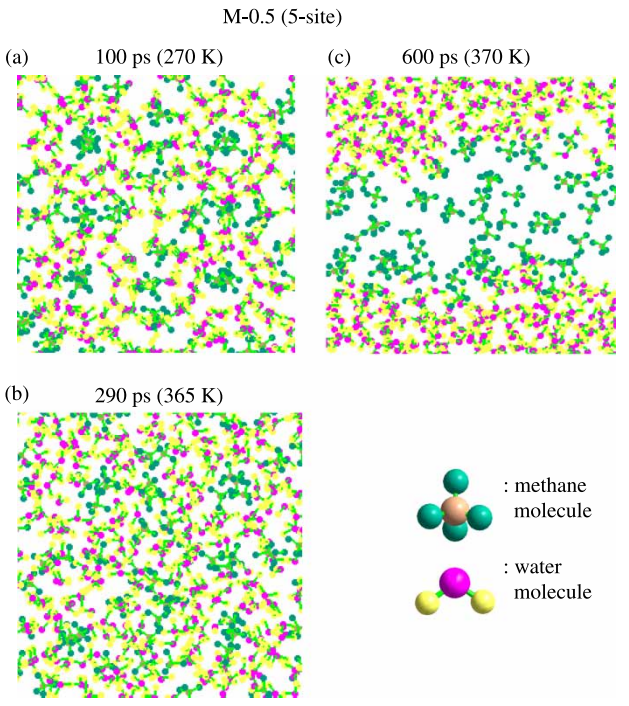

Figure 3. Snapshots of MD simulation for CH_4 hydrate dissociations with the 5-site model ($\Delta T = 0.5$ TK/s).

radial distribution functions for methane were observed at about 7.5 Å and the hydrate was formed. The peaks with the 5-site model were slightly broader and lower than those with the TraPPE model. This means that the methane molecules with the 5-site move in wider space in hydrate cages than those with the TraPPE model. Figure 4(b) shows the water (oxygen atom)–water (hydrogen atom) radial distribution functions. The first peaks represent hydrogen atoms in own molecules. The second peaks represent the hydrogen bond. The radial distribution functions with two models were very similar. The structures of water were not influenced by the potential models of guest methane molecules. Figure 4(c) shows the radial distribution functions for methane after dissociation at 370 K. The shapes of the radial distribution functions in the figure were very similar to those in Figure 1 except for the heights. The peak heights depend on the fluid densities. It is shown that many methane molecules moved out from the cages and made a fluid-like structure. Figure 4(d) shows the radial distribution functions of water at 370 K with the two potential models of methane. It is found that water molecules made liquid phase at the condition. As shown in Figure 2(b) and (c), the cell length with the TraPPE model was 26.5 Å and that with the 5-site model was 28.5 Å at 370 K. The cell volume with the 5-site model was 1.24 times larger than that with the TraPPE model at 370 K. As shown in Equation (3), the radial distribution function is a function of volume. If one divides the radial distribution function with the 5-site model by 1.24, the results become very similar to the radial distribution function with the TraPPE model. This means that the structures of water in methane+water mixture with the two potential models of methane were very similar. The above results mentioned that the potential models of methane molecule did not much

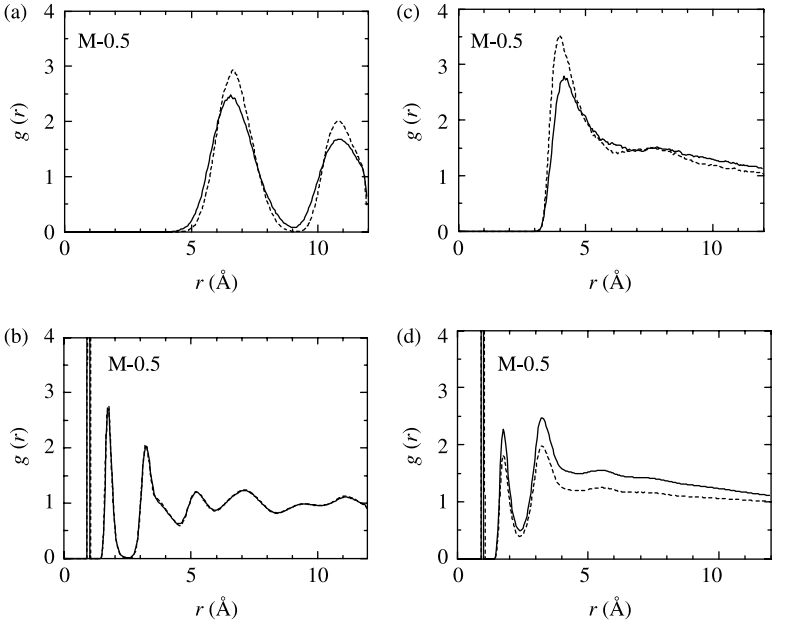

Figure 4. Radial distribution functions of CH_4 hydrate ($\Delta T = 0.5$ TK/s). (a) Methane–methane from 60 to 100 ps at 270 K; (b) water(O)–water(H) from 60 to 100 ps at 270 K; (c) methane–methane from 560 to 600 ps at 370 K and (d) water(O)–water(H) from 560 to 600 ps at 370 K; (—) 5-site model; (- - -) TraPPE model.

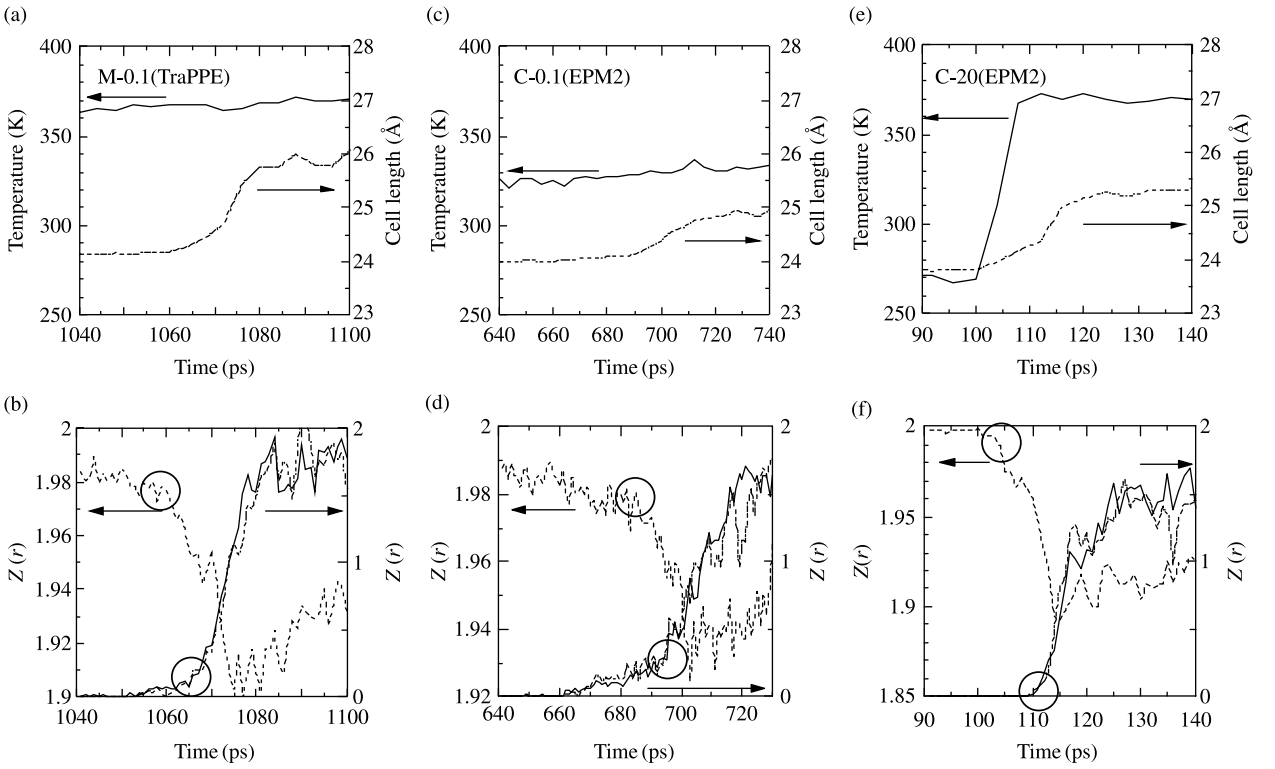

Figure 5. (a,c,e) Temperature profiles and cell lengths. (a) CH_4 hydrate, $\Delta T = 0.1$ TK/s; (c) CO_2 hydrate, $\Delta T = 0.1$ TK/s; (e) CO_2 hydrate, $\Delta T = 20$ TK/s; (—) temperature profile; (- - -) cell length. (b,d,f) Coordination numbers. (b) CH_4 hydrate, $\Delta T = 0.1$ TK/s; (d) CO_2 hydrate, $\Delta T = 0.1$ TK/s; (f) CO_2 hydrate, $\Delta T = 20$ TK/s; (- - -) H_2O (H—O); (—) M-cage gas; (– – –) S-cage gas.

influence the dissociation process of methane hydrate. To save the calculation times, it may be reasonable to adopt the TraPPE model to analyse the dissociation process of methane hydrate. The authors used only the TraPPE model for methane in the flowing sessions.

5.5 *Coordination numbers*

The simulated results of coordination numbers for guest gases and water molecules are shown in Figure 5. The integration ranges are 2.55, 4.35 and 4.25 Å for water, methane and carbon dioxide molecules, respectively. The integration ranges of methane and carbon dioxide molecules were determined from the start positions of the first peaks of radial distribution functions for CH_4 and CO_2 hydrates at 270 K, respectively. The integration range of water was determined from the end position of the second peak of radial distribution functions for water at 270 K. The start points to dramatically decrease the coordination number for water and those to increase the coordination number for guest gases are shown by circles in Figure 5(b), (d) and (f). For all systems, the points that dramatically decreased the coordination number of water molecules are earlier than those that increased the coordination number of gas molecules. This means that the water cages break down first, and then the guest gases get out from the cages.

5.6 *Mean square displacements*

Figure 6 shows the mean square displacements during the start times for dissociations. The slopes of the mean square displacements of guest gases and water during the start times for dissociation are listed in Table 2. As shown in Table 2, the slopes of the mean square displacements of guest gases were smaller than those of water during the start times for dissociation. This means that the water cages break down first, and then the guest gases get out from the cages. The results are consistent with those from the coordination numbers. The results were obtained for CH_4 and CO_2 hydrates with increasing temperature. The results are consistent with the results by Ding et al. [7] for CH_4 hydrate simulation at constant temperatures.

6. Conclusion

The dissociation processes for methane and carbon dioxide hydrates were investigated by MD simulation with increasing temperature. The TraPPE (single-site) and

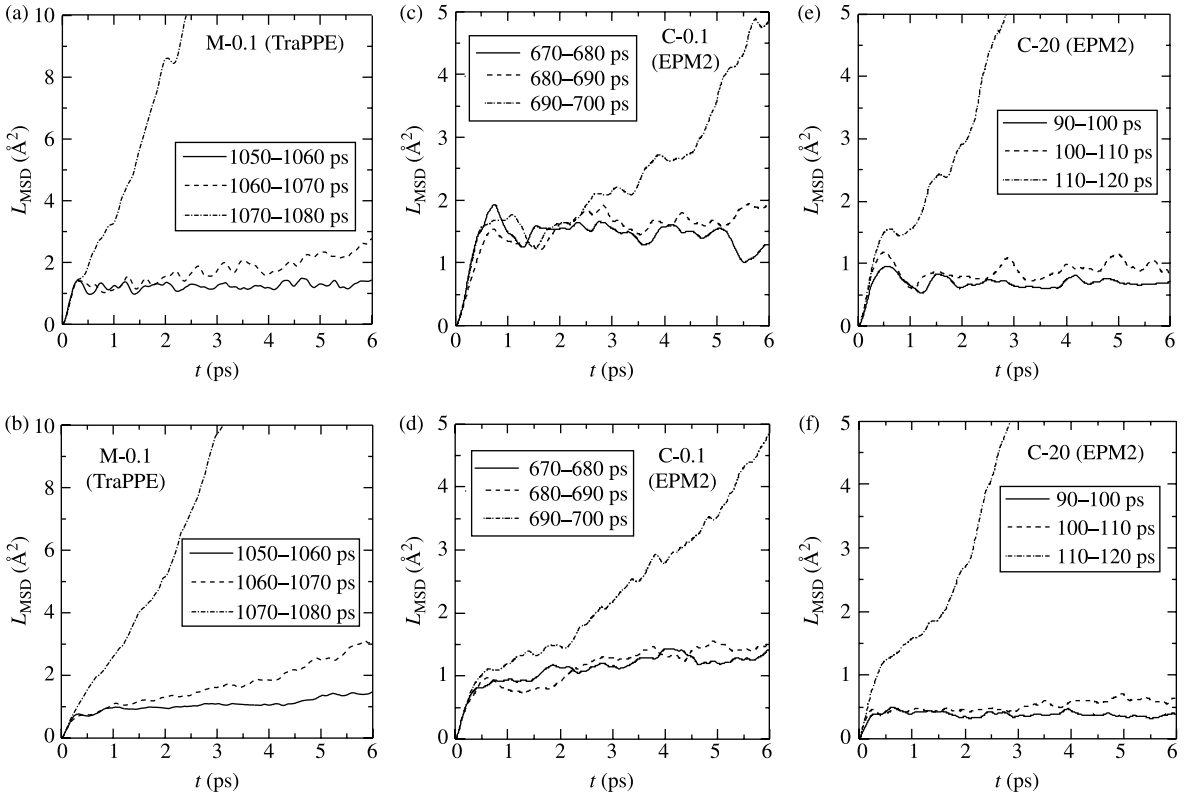

Figure 6. Mean square displacements L_{MSD}. (a) Methane molecules for CH_4 hydrate, $\Delta T = 0.1$ TK/s; (b) water molecules for CH_4 hydrate, $\Delta T = 0.1$ TK/s; (c) carbon dioxide molecules for CO_2 hydrate, $\Delta T = 0.1$ TK/s; (d) water molecules for CO_2 hydrate, $\Delta T = 0.1$ TK/s; (e) carbon dioxide molecules for CO_2 hydrate, $\Delta T = 20$ TK/s and (f) water molecules for CO_2 hydrate, $\Delta T = 20$ TK/s.

Table 2. Slopes of the mean square displacements of guest and water molecules from 0.5 to 6 ps during start times of dissociations.

		Slope × 10^2 (Å^2/ps)	
Condition	Period (ps)	Guest	Water
M-0.1 (TraPPE)	1050–1060	3.0	10.0
C-0.1 (EPM2)	680–690	8.1	14.6
C-20 (EPM2)	100–110	3.2	4.4

5-site models were adopted for methane molecules. The potential models of methane molecule did not much influence the dissociation process of methane hydrate. Methane hydrate was more stable than carbon dioxide hydrate at the calculated conditions with the potentials adopted in this work. The points that dramatically decreased the coordination number of water molecules were earlier than those that increased the coordination number of gas molecules. The slopes of mean square displacements for guest gas molecules were smaller than those for water molecules during the start times for dissociation process. The results mean that the water cages break down first, and then the gas molecules get out from the water cages.

References

[1] E.D. Sloan, Jr., *Clathrate hydrates of natural gases*, Marcel Dekker Inc., New York, NY, 1990.
[2] S. Hirai, K. Okazaki, S. Kuraoka, and K. Kawamura, *Study for the stability of CO_2 clathrate-hydrate using molecular dynamics simulation*, Energy Convers. Mgmt 37 (1996), pp. 1087–1092.
[3] S. Hirai, K. Okazaki, Y. Tabe, and K. Kawamura, *CO_2 clathrate-hydrate formation and its mechanism by molecular dynamics simulation*, Energy Convers. Mgmt 38 (1997), pp. S301–S306.
[4] J.S. Tse and D.D. Klug, *Formation and decomposition mechanisms for clathrate hydrates*, J. Supramol. Chem. 2 (2002), pp. 467–472.
[5] A.A. Chialvo, M. Houssa, and P.T. Cummings, *Molecular dynamics study of the structure and thermophysical properties of model sI*, J. Phys. Chem. B 106 (2002), pp. 442–451.
[6] N.J. English, J.K. Johnson, and C.E. Taylor, *Molecular-dynamics simulations of methane hydrate dissociation*, J. Chem. Phys. 123 (2005), 244503.
[7] L.Y. Ding, C.Y. Geng, Y.H. Zhao, and H. Wen, *Molecular dynamics simulation on the dissociation process of methane hydrates*, Mol. Sim. 35 (2007), pp. 1005–1016.
[8] E.M. Myshakin, H. Jiang, R.P. Warzinski, and K.D. Jordan, *Molecular dynamics simulations of methane hydrate decomposition*, J. Phys. Chem. A 113 (2009), pp. 1913–1921.
[9] S. Nose, *A molecular dynamics method for simulations in the canonical ensemble*, Mol. Phys. 52 (1984), pp. 255–268.
[10] M. Parrinello and A. Rahman, *Polymorphic transitions in single crystals: A new molecular dynamics method*, J. Appl. Phys. 52 (1981), pp. 7182–7190.
[11] R.K. McMullan and G.A. Jeffrey, *Polyhedral clathrate hydrates. IX. Structure of ethylene oxide hydrate*, J. Chem. Phys. 42 (1965), pp. 2725–2732.

[12] P. Ewald, *The calculation of optical and electrostatic grid potential*, Ann. Phys. 64 (1921), pp. 253–287.
[13] M.G. Martin and J.I. Siepmann, *Transferable potentials for phase equilibria. 1. United-atom description of n-alkanes*, J. Phys. Chem. B 102 (1998), pp. 2569–2577.
[14] J.G. Harris and K.H. Yung, *Carbon dioxide's liquid–vapor coexistence curve and critical properties as predicted by a simple molecular model*, J. Phys. Chem. 99 (1995), pp. 12021–12024.
[15] H.J.C. Berendsen, J.R. Grigera, and T.P. Straatsma, *The missing term in effective pair potentials*, J. Phys. Chem. 91 (1987), pp. 6269–6271.
[16] J.R. Errington and A.Z. Panagiotopoulos, *A fixed point charge model for water optimised to the vapor–liquid coexistence properties*, J. Phys. Chem. B 102 (1998), pp. 7470–7475.
[17] J.R. Errington, G.C. Boulougouris, I.G. Economou, A.Z. Panagiotopoulos, and D.N. Theodorou, *Molecular simulation of phase equilibria for water–methane and water–ethane mixtures*, J. Phys. Chem. B 102 (1998), pp. 8865–8873.
[18] U. Setzmann and W. Wagner, *A new equation of state and tables of thermodynamic properties for methane covering the range from the melting line to 625 K at pressures up to 1000 MPa*, J. Phys. Chem. Ref. Data 20 (1991), pp. 1061–1155.